A co-assembly system of an aromatic donor and acceptor: charge transfer, electric bistability and photoconductivity†

Jia Luo,[a] Linfeng Chen,[a] Jie-Yu Wang,[b] Ting Lei,[b] Li-Yi Li,[b] Jian Pei*[b] and Yanlin Song*[a]

Received (in Montpellier, France) 9th July 2010, Accepted 24th August 2010
DOI: 10.1039/c0nj00536c

A co-assembly system organized through the interaction between an aromatic donor and an acceptor was developed, in which the charge transfer (CT) process taking place proved to be a key point for achieving both electric bistability and photoconductivity. This strategy is instructive for constructing "bottom-up" systems and functional devices based on the CT principle from such a co-assembly system of donor and acceptor.

Charge transfer (CT) from an electron donor (D) to an acceptor (A) is a basic process in biological and artificial photosynthesis.[1] Recently, many organic CT systems have been shown to exhibit potential applications in opto-/electronic devices such as in photovoltaic cells[2] and electrical data storage.[3] Organic CT systems with a good performance in electrical data storage need bistability ("0" and "1" states), generally corresponding to low/high electric conductivity, in which CT between organic electron donor and acceptor units renders a high conductivity transition up to the threshold voltage.[3c–f] For example, non-volatile flash memory devices exhibit the reversibility of a CT process under an electric field. Although CT in a single D–A molecule[3e] and D–A mixture[3f] has been considerably investigated, both the inevitable intramolecular CT state in the former and the phase separation in the latter cause less than stable device performance. Therefore, to develop new ordered D–A co-assembly systems is still a challenge to obtain excellent electrical bistable devices,[4] in which effective intermolecular CT and a lower phase separation tendency are remarkably favored. Moreover, the investigation of such co-assembly systems and their CT processes further promotes the study of electrical data storage.

Herein, to realize functionality in a co-assembled D–A system for optoelectronic devices, we have developed two complementary aromatic donor and acceptor molecules, and present their electrical bistability and photoconductivity behaviors based on a CT process. Fig. 1 illustrates the molecular structures of the electron donor (**Tr**) and the acceptor (**TrO$_3$**). This two-component system exhibits strong π–π interactions, and an obvious one-dimensional (1D) co-assembly (**Tr**:**TrO$_3$**) features in solution, in the solid state and even in the mesophase.[5] An investigation of the optical and electrical properties indicates that intermolecularly stable CT happens due to a highly ordered donor and acceptor arrangement. We also achieved an intermolecular CT-based photoconductivity behavior from the 1D co-assemblies constructed through the intermolecular π–π stacking force.

To understand the HOMO/LUMO distribution of **Tr** and **TrO$_3$**, theoretical calculations were performed by density functional theory (DFT) using the B3LYP/6-311+G(d,p)//B3LYP/6-31G(d) level.[6] Fig. S1† shows the HOMO and LUMO distribution of **Tr** and **TrO$_3$**, calculated by DFT. The results indicate that both the HOMO level of **Tr** and the LUMO level of **TrO$_3$**, distributed over the whole planar conjugated skeleton, favor co-assembly and CT from donor to acceptor. The X-ray diffraction (XRD) pattern (Fig. 2a–c) of the complex (**Tr**:**TrO$_3$**) in a film exhibits a main sharp reflection peak with a *d* spacing of 1.62 nm and another weak peak with a spacing of 0.35 nm, corresponding to the distance of typical interplanar π–π stacking. Compared with that of the individual **Tr** and **TrO$_3$** units, the XRD pattern of the complex shows a different crystalline mode through co-assembly between the π-conjugated donor and acceptor molecules, as seen by an analysis of the small angle reflections (1.54 and 2.10 nm for **Tr** and **TrO$_3$**, respectively). The co-assembly behavior was also investigated using a scanning tunneling microscope (STM). In a simple self-assembly manner, the solution of the complex in CH_2Cl_2 (5×10^{-7} M) was deposited onto highly oriented pyrolysis graphite (HOPG) by drop-casting. Fig. 2d illustrates current STM images of **Tr**:**TrO$_3$** in the thin film. The D/A molecules were arranged periodically on the surface with lattice constants of a = 2.1 and b = 2.0 nm, and θ = 124°, which is consistent with the diameter of the molecules (*ca.* 2.8 nm, containing extended flexible chains). Therefore, the alkyl chains adopt to some extent a staggered conformation on the HOPG surface.

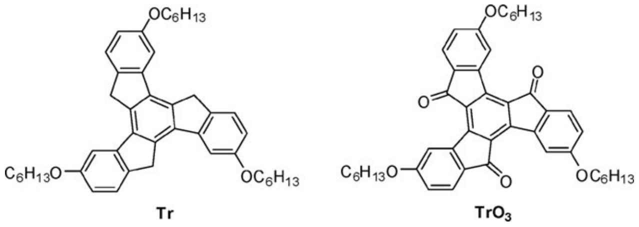

Fig. 1 Molecular structures of the complementary donor **Tr** and acceptor **TrO$_3$**.

---

[a] *Beijing National Laboratory for Molecular Sciences (BNLMS), Key Laboratory of Organic Solid, Laboratory of New Materials, Institute of Chemistry, The Chinese Academy of Sciences, Beijing 100190, China. E-mail: ylsong@iccas.ac.cn*
[b] *Beijing National Laboratory for Molecular Sciences, The Key Laboratory of Bioorganic Chemistry and Molecular Engineering of the Ministry of Education, College of Chemistry, Peking University, Beijing 10087, China. E-mail: jianpei@pku.edu.cn; Fax: +86 10 62751708*

† Electronic supplementary information (ESI) available: Experimental procedures and details. See DOI: 10.1039/c0nj00536c

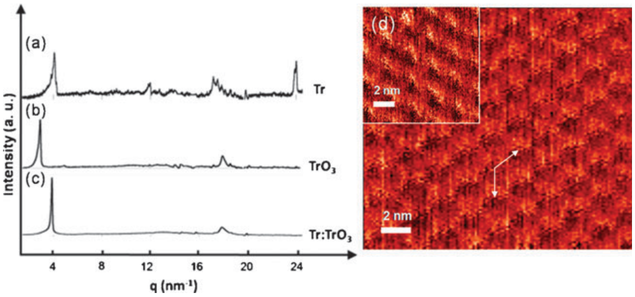

Fig. 2 X-Ray diffraction pattern of (a) **Tr**, (b) **TrO$_3$** and (c) 1 : 1 **Tr**:**TrO$_3$** in films. (d) STM image of a co-assembled **Tr**:**TrO$_3$** film on HOPG. Scanning conditions: V_{bias} = 0.43 V, I_{ref} = 0.10 nA. The inset shows the STM current image at a different position.

Furthermore, to investigate the CT properties of such a co-assembly system, we first constructed a thin film device with a two-end structure of ITO/**Tr**:**TrO$_3$**/Al to test its electrical bistability behavior. The electroactive layer (*ca.* 100 nm) was prepared by spin-coating a solution of **Tr**:**TrO$_3$** in CHCl$_3$ (30 mg mL^{-1}). Fig. 3 shows the typical reversible bistability characteristics of this device during voltage sweeping. As depicted in curve **1**, the first voltage, scanning from 0 to 2.4 V, showed a sharp current increase at about 1.6 V, corresponding to the transition from a low conductivity state ("0") to a high conductivity state ("1"). The on/off ratio extracted from the logarithm coordinates (Fig. 3 inset) was close to 10^2. Subsequently, the second scanning (curve **2**), from 0 to 2.4 V, reflected the "on" state of the device. A reverse voltage (curve **3**) scanning led to a current fall at a threshold of −2.0 V, and finally the device was turned "off" at a current level of 10^{-7} A (curve **4**). The *I–V* curve remained stable during iterative scanning once the device had been turned on. Obviously, the electrical bistability was not controlled by a metallic filament mechanism because of the apparently low on/off ratio[7] (10^2). To understand the role of the D–A interaction in this bistable device, a single-component control device was fabricated, and no conductivity transition appeared in the range 0 to 3 V (Fig. S4†). Furthermore, a double-layer device with the structure ITO/**TrO$_3$**/**Tr**/Al was fabricated, which demonstrated that the electrical bistability existed only in the D–A system (Fig. S5†). Reasonably, the CT process from the donor to the acceptor under an appropriate applied voltage led to a high electrically conductive state of the system, discriminated from its ground state.[3d,e] As depicted in Fig. 4a, time-dependent UV-vis absorption spectra under a 3 V bias showed an obvious absorption intensity enhancement of the long wavelength bands, assigned as a transition of the CT state.[3c] The CT state can be preserved for up to 24 h under ambient conditions. In addition, this effect can be erased by applying a reverse voltage of −2.5 V (Fig. S6†), demonstrating the reversible nature of CT.

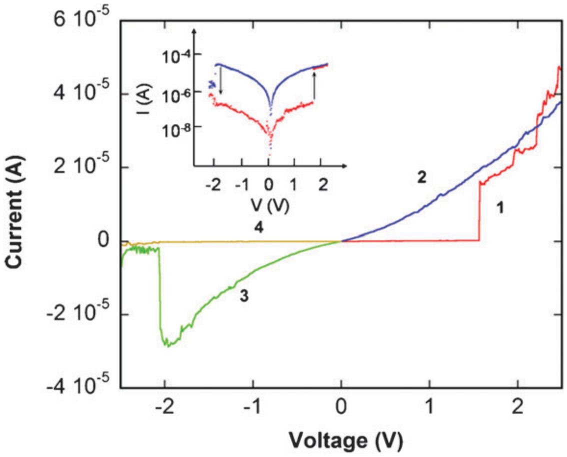

Fig. 3 *I–V* characteristics of the device with the structure ITO/**Tr**:**TrO$_3$**/Al. The scanning results showed the conductance transition from the low- to the high-conductivity state in curve **1**, the memory effect of the high-conductivity state in curve **2**, and the recovery of the low-conductivity state with the application of a reverse voltage scan in curves **3** and **4**. The inset demonstrates the current transition logarithmically.

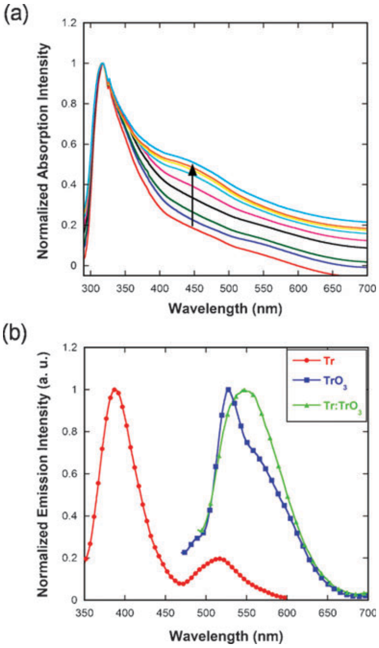

Fig. 4 (a) UV-vis absorption spectra of a **Tr**:**TrO$_3$** in film under a 3 V bias. The spectra were recorded at 10 s intervals. (b) Emission spectra of **Tr**, **TrO$_3$** and **Tr**:**TrO$_3$** films.

The HOMO/LUMO energy levels of the two molecules were estimated by the cyclic voltammetry method to be −5.13/−3.02 eV (**Tr**) and −6.22/−3.32 eV (**TrO$_3$**), respectively. Hence, CT in the excited state occurred with a low energy barrier. Fig. 4b shows their emission spectra in films, and the red-shifted emission peak at a wavelength of 550 nm proved to be a similar CT process to the complex film when excited by photons. Therefore, the co-assembly became a high-conductivity state once light illumination was applied. To investigate CT in the 1D co-assembly system produced by photons, as well as to consider the high conductivity state at the threshold voltage in thin films, devices based on self-assembled microwires were conducted with an electrode width of 20 μm, which led to a low electric field intensity that retained the system in the "off" state unless the microwires were illuminated. Scanning electron microscopy (SEM) images revealed the formation of self-assembled 1D microwires in

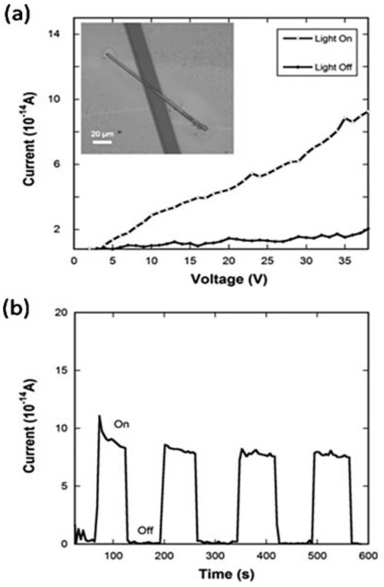

Fig. 5 The photoconductivity behavior of self-assembled microwires of **Tr**:**TrO$_3$**: (a) *I*–*V* characteristics under dark and light illumination; (b) photoswitching characteristics at a bias of 40 V. Light intensity = 318 mW cm^{-2}. The inset shows a typical two-ended device under an optical microscope.

hexane by using **Tr**, **TrO$_3$** and their 1 : 1 complex, respectively. Two-ended photoconductor devices using the **Tr**:**TrO$_3$** complex were fabricated by spin-casting a microwire suspension in hexane onto a treated SiO$_2$ substrate, followed by deposition of Au electrodes (50 nm). By using a mask during the deposition, an electrode gap of roughly 20 μm wide was achieved (Fig. 5a, inset). First, under dark conditions, the device produced a very low current (*ca.* 10^{-14} A), meaning an "off" state with a very low concentration of charge carriers. However, once the microwire was illuminated with UV light of a 365 nm wavelength, the current instantaneously increased by nearly a 1–2 order of magnitude, defining the "on" state. This transition was attributed to the photoexcited CT state[8] between the donor and the acceptor, similar to that of the electrically bistable state. The photoswitching effect was demonstrated by controlling the UV light on/off, as shown in Fig. 5b. The current remained stable at a level of 10^{-13} A during several on/off cycles. However, the microwires self-assembled by individual **Tr** or **TrO$_3$** units showed a weak effect under UV light illumination, with an on/off ratio of *ca.* 2–3 (Fig. S7†). This low response to UV light meant that there was no highly conductive CT state in any individual donor or acceptor molecule and that the photoconductivity was only derived from photogenerated carriers in the π-conjugated semiconductors.[9]

In conclusion, a co-assembly system containing an aromatic donor and acceptor has been developed to achieve both electrical bistability and photoconductivity. Its CT process has been investigated in detail by STM, optical spectra, XRD and thin film devices. The π–π stacking between the donor and the acceptor molecules results in ordered co-assemblies, either in films or in 1D microwires. Indeed, the alternative D–A arrangement ensures a stable CT and avoids phase separation in film formation, resulting in obvious electric bistability and photoconductivity behaviors. The co-assembly strategy *via* complementary donors and acceptors is of significance for constructing "bottom-up" systems and developing novel functional devices based on the CT principle.

We thank the NSFC (Grants nos. 50625312, U0634004 and 20421101) and the 973 program for their continued financial support. The Chinese Academy of Sciences is gratefully acknowledged. Dr Jia Luo gratefully acknowledges the support of the K. C. Wong Education Foundation, Hong Kong and a China Postdoctoral Science Foundation funded project.

Experimental

The compounds **Tr** and **TrO$_3$** were synthesized as per the procedure in our previous report.[5] Absorption spectra were recorded on a Perkin-Elmer Lambda 35 UV-vis spectrometer. Photoluminescent (PL) spectra were carried out on a Perkin-Elmer LS55 luminescence spectrometer. Optical microscopy was conducted with an Olympus BX-51 microscope. Scanning tunneling microscopy (STM) studies were performed with a Solver P47 apparatus under ambient conditions. The STM tips were made of electrochemically-etched tungsten.

Preparation procedure of microwires: samples were dissolved in boiling hexane (1 mg mL^{-1}) and cooled to room temperature. Then, the solid precipitated from the solution and was collected in the form of microwires.

Thin film device fabrication and testing

ITO glasses were cleaned by sonication in acetone for 10 min, followed by 5 min of ozone plasma exposure. Films of **Tr**, **TrO$_3$** and **Tr**:**TrO$_3$** were made by spin-coating their solutions in CHCl$_3$ (30 mg mL^{-1}) at a speed of 2000 rpm. Their thicknesses were 50 nm. For a double-layer device, the solution of **TrO$_3$** in CHCl$_3$ (30 mg mL^{-1}) was first spin-coating onto ITO glass; then, the film of **Tr** (30 nm) was fabricated by thermal evaporation under a pressure of 4×10^{-4} Pa at 0.5–1.0 Å s^{-1}. Then, a layer of 100 nm Al was deposited onto the films by thermal evaporation under a pressure of 4×10^{-4} Pa at 0.2–2.0 Å s^{-1}. *I*–*V* characteristics were tested in an ambient atmosphere using a Keithley 4200-SCS system.

Photoconductor fabrication and testing

300 nm-thick SiO$_2$ was thermally deposited onto the Si substrate. The substrates were cleaned by sonication in acetone for 10 min, followed by 5 min of ozone plasma exposure. Octyltrimethoxysilane self-assembled monolayer (SAM) deposition on SiO$_2$ was conducted using a previously reported procedure.[10] A polyethylene (PE) fiber with a diameter of 20 μm was mounted on the substrate as a shadow mask, and a layer of 50 nm gold was deposited onto the substrate by thermal evaporation under a pressure of 4×10^{-4} Pa at 0.3–1.0 Å s^{-1} before the fiber mask was removed. The photoconductor based on a single microwire was tested in an ambient atmosphere using a Keithley 4200-SCS system connected to a Vector BX4000 manual probe station. The irradiation light was provided by an Omron LED with a wavelength of 365 nm.

Notes and references

1 (*a*) M. R. Wasielewski, *Chem. Rev.*, 1992, **92**, 435; (*b*) D. Gust, T. A. Moore and A. L. Moore, *Acc. Chem. Res.*, 2001, **34**, 40; (*c*) F. D'Souza, P. M. Smith, M. E. Zandler, A. L. McCarty, M. Itou, Y. Araki and O. Ito, *J. Am. Chem. Soc.*, 2004, **126**, 7898.

2 (*a*) S. Günes, H. Neugebauer and N. S. Sariciftci, *Chem. Rev.*, 2007, **107**, 1324; (*b*) G. Yu, J. Gao, J. C. Hummelen, F. Wudl and A. J. Heeger, *Science*, 1995, **270**, 1789; (*c*) N. S. Sariciftci, L. Smilowitz, A. J. Heeger and F. Wudl, *Science*, 1992, **258**, 1474; (*d*) A. Nantalaksakul, A. Mueller, A. Klaikherd, C. J. Bardeen and S. Thayumanavan, *J. Am. Chem. Soc.*, 2009, **131**, 2727.

3 (*a*) G. Jiang, Y. Song and D. Zhu, in *High Density Data Storage—Principle, Technology, and Materials*, ed. Y. Song and D. Zhu, World Scientific Publishers, 2009, pp. 137–191; (*b*) Y. Yang, J. Ouyang, L. Ma, R. J.-H. Tseng and C.-W. Chu, *Adv. Funct. Mater.*, 2006, **16**, 1001; (*c*) H. Wu, Y. Song, S. Du, H. Liu, H. Gao, L. Jiang and D. Zhu, *Adv. Mater.*, 2003, **15**, 1925; (*d*) G. Jiang, T. Michinobu, W. Yuan, M. Feng, Y. Wen, S. Du, H. Gao, L. Jiang, Y. Song, F. Diederich and D. Zhu, *Adv. Mater.*, 2005, **17**, 2170; (*e*) Y. Wen, J. Wang, J. Hu, L. Jiang, H. Gao, Y. Song and D. Zhu, *Adv. Mater.*, 2006, **18**, 1983; (*f*) C. W. Chu, J. Ouyang, J.-H. Tseng and Y. Yang, *Adv. Mater.*, 2005, **17**, 1440.

4 J. H. Kim, S. V. Lindeman and J. K. Kochi, *J. Am. Chem. Soc.*, 2001, **123**, 4951.

5 J.-Y. Wang, J. Yan, L. Ding, Y. Ma and J. Pei, *Adv. Funct. Mater.*, 2009, **19**, 1746.

6 (*a*) M. J. Frisch, G. W. Trucks, H. B. Schlegel, G. E. Scuseria, M. A. Robb, J. R. Cheeseman, J. A. Montgomery, Jr., T. Vreven, K. N. Kudin, J. C. Burant, J. M. Millam, S. S. Iyengar, J. Tomasi, V. Barone, B. Mennucci, M. Cossi, G. Scalmani, N. Rega, G. A. Petersson, H. Nakatsuji, M. Hada, M. Ehara, K. Toyota, R. Fukuda, J. Hasegawa, M. Ishida, T. Nakajima, Y. Honda, O. Kitao, H. Nakai, M. Klene, X. Li, J. E. Knox, H. P. Hratchian, J. B. Cross, V. Bakken, C. Adamo, J. Jaramillo, R. Gomperts, R. E. Stratmann, O. Yazyev, A. J. Austin, R. Cammi, C. Pomelli, J. Ochterski, P. Y. Ayala, K. Morokuma, G. A. Voth, P. Salvador, J. J. Dannenberg, V. G. Zakrzewski, S. Dapprich, A. D. Daniels, M. C. Strain, O. Farkas, D. K. Malick, A. D. Rabuck, K. Raghavachari, J. B. Foresman, J. V. Ortiz, Q. Cui, A. G. Baboul, S. Clifford, J. Cioslowski, B. B. Stefanov, G. Liu, A. Liashenko, P. Piskorz, I. Komaromi, R. L. Martin, D. J. Fox, T. Keith, M. A. Al-Laham, C. Y. Peng, A. Nanayakkara, M. Challacombe, P. M. W. Gill, B. G. Johnson, W. Chen, M. W. Wong, C. Gonzalez and J. A. Pople, *GAUSSIAN 03 (Revision C.02)*, Gaussian, Inc., Wallingford, CT, 2004; (*b*) R. Dennington, T. Keith, J. Millam, K. Eppinnett, W. L. Hovell and R. Gilliland, *GaussView (Version 3.09)*, Semichem, Inc., Shawnee Mission, KS, 2003.

7 M. Feng, X. Guo, X. Lin, X. He, W. Ji, S. Du, D. Zhang, D. Zhu and H. Gao, *J. Am. Chem. Soc.*, 2005, **127**, 15338.

8 (*a*) Y. Yamamoto, T. Fukushima, Y. Suna, N. Ishii, A. Saeki, S. Seki, S. Tagawa, M. Taniguchi, T. Kawai and T. Aida, *Science*, 2006, **314**, 1761–1764; (*b*) Y. Yamamoto, T. Fukushima, A. Saeki, S. Seki, S. Tagawa, N. Ishii and T. Aida, *J. Am. Chem. Soc.*, 2007, **129**, 9276.

9 (*a*) Y. S. Cohen, S. Xiao, M. L. Steigerwald, C. Nuckolls and C. R. Kagan, *Nano Lett.*, 2006, **6**, 2838; (*b*) A. D. Schwab, D. E. Smith, B. Bond-Watts, D. E. Johnston, J. Hone, A. T. Johnson, J. C. de Paula and W. F. Smith, *Nano Lett.*, 2004, **4**, 1261.

10 Y. Ito, A. A. Virkar, S. Mannsfeld, J. H. Oh, M. Toney, J. Locklin and Z. Bao, *J. Am. Chem. Soc.*, 2009, **131**, 9396.